

# STRUCTURAL PERFORMANCE OF HIGH CAPACITY GLULAM MOMENT CONNECTIONS

Ryan Guay <sup>1</sup>, Christopher Pitt <sup>2</sup>, Reid B. Zimmerman <sup>3</sup>, Ignace Mugabo <sup>4</sup>, Peter Dusicka <sup>5</sup>

**ABSTRACT:** Moment connections in glulam members are desirable over simple connections to increase load-carrying capacity and reduce deflections for the same glulam cross section. However, moment connections in glulam members often result in a large tension-compression couple. To achieve high tension capacity, a large number of fasteners acting in dowel shear are often utilized. Brittle failure modes such as block shear and group tear-out can dominate such connections.

This study evaluates the structural performance of high capacity glulam moment and tension connections in two configurations based on the results of physical testing: (1) Steel plates installed with 90-degree screws on both of the outer, side faces of a glulam member, and (2) two steel plates nested into a glulam member and installed with self-drilling dowels. Calculation-based results and physical load test results are compared. The results from this study show that block shear capacity estimations as adopted in design standards may be unconservative for high capacity moment or tension connections. A potential modification through perpendicular-to-grain reinforcing screws to help mitigate the block shear failure is presented. Further research on high capacity moment and tension connections is needed to provide better agreement between design versus actual capacity, especially for block shear type failure modes.

**KEYWORDS:** Glulam Connections, Self-Drilling Dowels, Wood Screws, Block Shear Failure, Reinforcing Screws

## 1 INTRODUCTION

Glulam connections commonly used in buildings in North America are configured as simple shear connections with negligible capacity to resist bending moments. Glulam moment connections are uncommon, particularly in cases where high capacities are required. In order to achieve the long-span glulam beams, cantilevers, and wood-steel hybrid structure desired for the new Portland International Airport Terminal Core Redevelopment (TCORE) roof located in Portland, Oregon, USA, high capacity moment connections were developed for deep glulam beams. This paper evaluates dowel-type glulam moment connections using a multi-scale approach and a comparison between test and analytical results. The paper also presents a solution for mitigating premature block shear failures in such connections.

### 1.1 Background for timber connection testing

The Port of Portland's TCORE project is a roughly \$2 billion terminal redevelopment project, including an approximately 300 m x 120 m mass timber hybrid roof with approximately 6 m wide x 2 m deep paired steel plate girder sections spaced at 30 m. Approximately 170 mm

wide x 2 m deep x 24 m long Douglas-fir glulam beams span perpendicular to the steel plate girders at 3 m spacing. The roof structure is seismically isolated with curved surface slider (friction pendulum) isolators located at the top of the Y-column connections to the bottom of the steel plate girders [1]. This requires that the glulam beams transmit seismic loading from the roof diaphragm above to the isolation plane below through strong-axis bending. Additionally, glulam beams support roof edge cantilevers of over 10 m and are optimized by functioning as continuous beams with moment connections to the plate girders. Due to the large demands and unique nature of these connections, an effort was made early in design to perform physical load testing of various connection configurations to develop a thorough understanding of their capacities and failure mechanisms.

Allowing for expansion and shrinkage in the glulam beams due to variations in moisture content (MC) during construction and service was a critical consideration. Excessive moisture content change and/or excessive restraint introduced by the dowel-connected steel plate connections could have resulted in wood splitting, compromising the capacity of the connection. Design to prevent splitting pursued limiting the perpendicular-to-

<sup>1</sup> Ryan Guay, KPFF Consulting Engineers, United States, Ryan.Guay@kpff.com

<sup>2</sup> Christopher Pitt, KPFF Consulting Engineers, United States, Christopher.Pitt@kpff.com

<sup>3</sup> Reid B. Zimmerman, KPFF Consulting Engineers, United States, Reid.Zimmerman@kpff.com

<sup>4</sup> Ignace Mugabo, Formerly of KPFF Consulting Engineers, United States

<sup>5</sup> Peter Dusicka, Portland State University, United States, dusicka@pdx.edu

grain distance between outer rows of fasteners connecting steel and glulam to a maximum of 150 mm, and separating the beam end tension/compression connections so they can each move independently in the vertical (perpendicular to grain) direction with the glulam beam end. Due to the critical nature of these connections, moisture cycling was performed on selected specimen followed by load testing, to verify that no significant reduction in capacity occurred due to moisture cycling.

### 1.2 Brief introduction to general testing approach

To develop the proposed connection configurations, the roof structure was analysed to determine the various levels of tension/compression demand required near the top and bottom of glulam beams to provide bending moment resistance at the beam ends. A data binning approach was used to group various levels of glulam demands to minimize the number of different connections required on the project, while also achieving efficiency in the design. Beam vertical shear demands are resisted by direct bearing of bottom of glulam beams on steel plate girder, not through dowel fasteners.

Analyses determined that (3) connection capacity levels were needed to efficiently meet the loading requirements for this project. Two proposed connection configuration options were explored. Both connection configurations were tested at all capacity levels, equalling (6) connection types, with (2) additional sub-types tested, for a total of (8) unique tested configurations.

Both beam bending specimen tests and smaller axial tension specimen tests were performed on the connection types, with the connections tested at full scale in both cases. The as-constructed connections in the TCORE roof are shown in photo 1 below.



Photo 1: As constructed glulam beam end moment connections

## 2 MATERIALS, METHODS, AND DATA PROCESSING

### 2.1 Description of timber connections

Two connection configuration design concepts were included in the testing program for the glulam beam end top/bottom moment connections; one consisted of a

connection composed of exposed 6 mm thick steel side plates with 6 mm x 90 mm wood screws installed each side, loaded in single shear. The other consisted of a connection composed of a pair of 6 mm thick steel plates slotted into and concealed within the width of the glulam beam, with 6 mm diameter self-drilling dowels (SDDs) installed through the glulam thickness and both steel plates, loaded on 4-shear planes. See figure 1 below for a graphical representation of the two concepts, along with the various sizes for the connection test configurations and fastener quantity. The left side of figure 1 indicates the external steel side plates with screws connection; the right side of figure 1 indicates the internal steel plates with self-drilling dowels connection.

All glulam specimens were made of Douglas-Fir (*Pseudotsuga menziesii*) timber with a 16.5 MPa tension lam bending stress grade. Specimens were kept at moisture content of 12% +/- 4% during fabrication and load testing of the connections. Four specimens were moisture cycled prior to load testing to study the effects that weather exposure and drying may have on the capacity of the connections. The steel side and thru-plates consisted of 6 mm thick ASTM A572 Grade 50 steel.

The larger type C3 and C6 connection test specimens differed from the connections used in the project in that the test specimens had a single large plate, whereas the project connections used two separate plates to prevent restraint during moisture shrinkage/expansion.

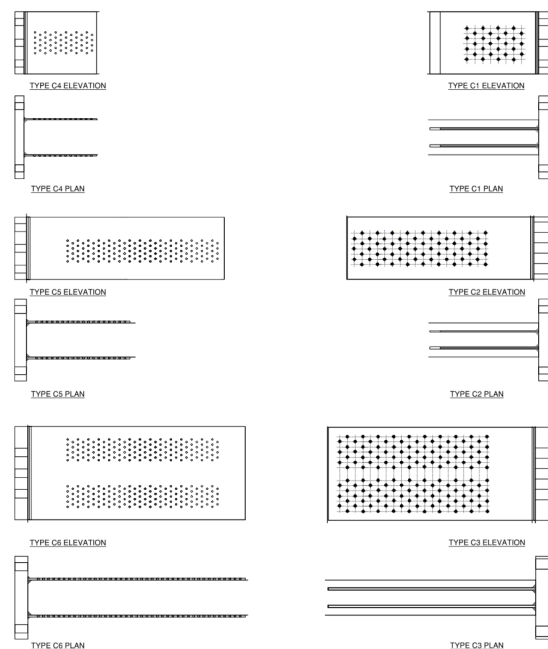


Figure 1: Summary of Connection Types Tested

### 2.2 Methods of testing

KPFF worked directly with Portland State University to utilize the infrastructure Testing and Applied Research

(iSTAR) Laboratory to perform the specimen load testing, which included both axial tension connection tests and beam bending tests. The specimens were fabricated off site by the same wood subcontractor as would be fabricating the project connections and shipped to the iSTAR Laboratory. A minimum of (8) connection tests were performed for each of the connection types. This number of tests was selected to balance cost/time of testing with the need to collect an adequate data set for performing limited statistical analysis.

Moisture content (MC) cycling testing followed by load testing on an additional (4) axial tension specimens was also performed. MC cycling was conducted in an environmental chamber at Oregon State University after which specimens were shipped to the iSTAR Laboratory for identical load testing to non-MC cycled specimens.

### 2.2.1 Physical Testing

A total of (28) axial tension specimen tests were performed, (12) tests using the 6 mm SDDs and (16) with the 6 mm x 90 mm wood screws. Following the completion of the axial tension specimen tests, (12) full scale bending specimen tests were performed, (6) using the 6 mm SDDs and (6) with the 6 mm x 90 mm wood screws. Douglas-fir glulam beams were used with the fasteners installed in laminations of equal or lower grade from those present at end connection locations in the project final condition. Steel test rig frames were fabricated to enable hydraulic jacks to apply loading to the specimens, with pressure/load and movements continuously monitored. The tension specimen tests were subjected to direct, concentric axial tension by pulling the two ends of the glulam specimen apart. The beam bending test specimens were subjected to shear and flexure by securing one end of the beam to the stationary test rig with a vertical shear bearing and horizontal compression connection bucket at the top and horizontal tension connection at the bottom, with a vertical upward load applied to the far end of the beam to induce shear and bending proportional with the actual roof demands. The beam bending specimens were each tested twice, with a tension connection installed at diagonally opposite corners to allow them to be flipped and rotated for testing after failure of the initially tested connection.

The connections were instrumented by the iSTAR Laboratory staff with load cells and deformation sensors. Deformation sensors measured deformation across the connection, rather than the entire specimen, directly. As a backup to the load cells for measuring force, pressure sensors for the hydraulic jacks were also present.

The axial tension specimen tests were performed first, which helped direct the path for the remaining tests by revealing which failure mechanisms should be more closely investigated. The axial tension specimen tests were quasi-statically loaded up to the approximate allowable stress design (ASD/service level) loads estimated from preliminary roof structure analyses, the

load was held for 10 minutes, and then the connections were quasi-statically loaded to failure. The loading to failure procedure was based on ASTM D1761-12 [2], which is typically used for determining the lateral load resistance for wood screws in the U.S. For each of the axial tension specimen tests, the same connection configuration was installed on each end of the glulam. The measured capacity of whichever end connection failed first was conservatively used as the capacity for both end connections and treated as two equal data points in the data analysis.

The beam bending specimen tests were loaded in a similar manner to the axial tension specimen tests with the exception of one full beam specimen that was loaded and held for a full 24 hour period at the ASD/service load. The objective of this test was to determine if any additional creep occurred during the hold period. See figure 2 for the test setup for representative specimens.

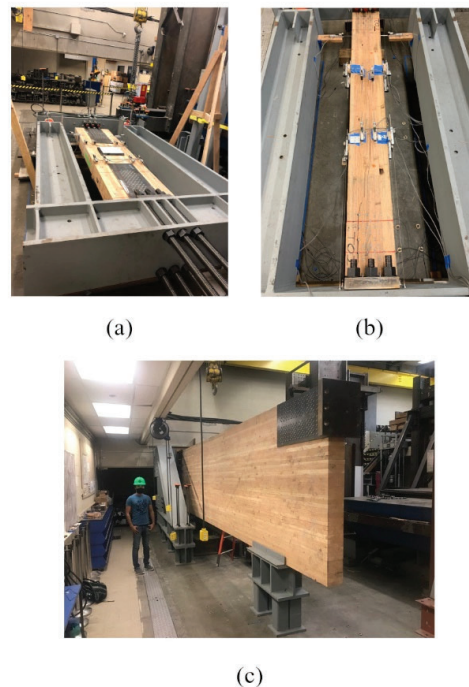


**Figure 2: Connection testing setup (a) tension specimen with external steel plates and wood screws, (b) tension specimen with internal steel plates and self-drilling dowels, and (c) bending specimen.**

### 2.2.2 Moisture Testing

To determine whether the proposed connection types were sensitive to wetting/drying (and associated wood shrinkage/expansion) after installation, moisture content (MC) cycling was applied to (4) axial tension test specimens prior to load testing. This was considered important because, in the actual project, the glulam beams would be exposed to weather during some phases of

construction despite best efforts to minimize such exposure through a detailed weather protection plan. For this testing, the connections were installed in glulam beams with industry standard 15%-16% MC, which aligned with the maximum MC allowed by project specifications. Pinned moisture monitors were installed to approximately 75 mm depth to measure internal MC before the glulam beam test specimens were placed in an environmental chamber at Oregon State University. Within the chamber, the temperature and humidity were controlled to cause expedited MC variations. The specimens were periodically sprayed with water for several days under low temperature and high humidity conditions until they increased to 22-27% MC (an increase of 6-12% MC). Then the chamber was set to higher temperature and low relative humidity to induce rapid drying. These conditions were maintained for over 4 weeks until the specimens reduced to 8-13% MC (a decrease of up to 16% MC from peak after wetting). See figure 3.

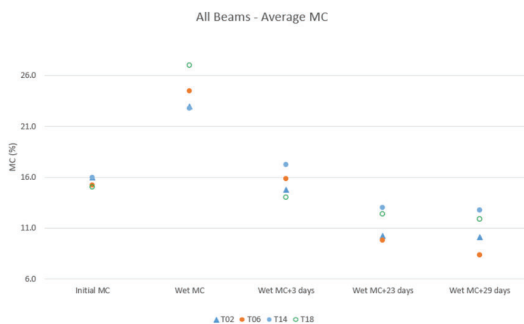


**Figure 3: Moisture content (MC) cycling data of glulam specimens**

Project specifications included requirements for moisture control and monitoring, which were calibrated to the MC testing performed. These included a maximum MC at time of connection installation, periodic monitoring of glulam beam MC after installation, and a maximum MC allowed at any point in construction. This ensured that the maximum variations in MC for in-situ project conditions were within those evaluated by testing. Final long-term minimum MC in the occupied building is estimated as 8% MC or above based on conservative assumptions of service temperature and relative humidity inside the conditioned building.

### 2.3 Statistical analysis of test results

To establish design capacities of the load tested connections, KPFF worked with the permitting authority for the project (The City of Portland, Oregon, Bureau of Development Services). Statistical analysis of the load test results following ASTM D2915-17 [3] established a nominal capacity for design on the basis that the physical testing methods for the connections were aligned with those of ASTM D1761-12 [2] and ASTM D5764-97a [4]. These latter ASTM standards are both typically used for

testing of mechanical fasteners and dowel-bearing strength in wood products in the U.S.

With the data that was collected from the tests, a 75% confidence level, one-sided tolerance limit, and population content of 95% were chosen (indicating that 95% of the population lies above the tolerance limit, 75% of the time through sampling). This confidence level, tolerance limit, and population content are the traditional approach for establishing structural capacities of wood products in the U.S. (i.e., 5% exclusion of lower capacities).

See Section 3.1 for a summary of the results. A graphical representation of the design capacity compared with the test data for each of the different types of connections is shown in figure 6.

### 2.4 NDS and Eurocode Calculations

In advance of performing the physical tests, calculations were made utilizing fastener manufacturer listed capacities, the design provisions of Appendix E of the American Wood Council's National Design Specification (NDS) for Wood Construction [5], and Annex A of Eurocode 5 [6] to determine expected design capacities. For block shear calculations (named as group tear-out in the NDS), the NDS equations consider the sum of the resistance from both the shear and tension portions of a potential failure perimeter. In contrast, Eurocode only takes the larger of the shear or tension portion capacity. See figure 4. This represents a fundamental difference in philosophy between the NDS and Eurocode. Where the NDS appears to assume load-sharing between the shear and tension portions of a block shear perimeter up to ultimate failure, Eurocode appears to assume that failure will occur on either the shear or tension portion but not both simultaneously. In other words, Eurocode appears to consider the differing deformations at failure between the shear and tensions portions whereas the NDS either neglects this or assumes some ductility in the portion which reaches capacity first.

Figure 4 below excerpts the relevant equations from NDS and Eurocode for comparison. See Section 3.2 for a comparison of load test results to calculations from both codes.

### E.4 Group Tear-Out Capacity

The adjusted tear-out capacity of a group of “n” rows of fasteners can be estimated as:

$$Z_{GT}' = \frac{Z_{RT-1}'}{2} + \frac{Z_{RT-n}'}{2} + F_t' A_{group-net} \tag{E.4-1}$$

where:

- $Z_{GT}'$  = adjusted group tear-out capacity
- $Z_{RT-1}'$  = adjusted row tear-out capacity of row 1 of fasteners bounding the critical group area
- $Z_{RT-n}'$  = adjusted row tear-out capacity of row n of fasteners bounding the critical group area
- $A_{group-net}$  = critical group net section area between row 1 and row n

(a)

#### Annex A (Informative): Block shear and plug shear failure at multiple dowel-type steel-to-timber connections

(1) For steel-to-timber connections comprising multiple dowel-type fasteners subjected to a force component parallel to grain near the end of the timber member, the characteristic load-carrying capacity of fracture along the perimeter of the fastener area, as shown in Figure A.1 (block shear failure) and Figure A.2 (plug shear failure), should be taken as:

$$F_{t,Rk} = \max \begin{cases} 1.5 A_{net,i} f_{t,0,k} \\ 0.7 A_{net,v} f_{v,k} \end{cases} \tag{A.1}$$

with

$$A_{net,i} = L_{net,i} t_i \tag{A.2}$$

$$A_{net,v} = \begin{cases} L_{net,v} t_i & \text{failure modes (c, f, j, l, k, m)} \\ \frac{L_{net,v}}{2} (L_{net,i} + 2t_e) & \text{all other failure modes } \text{\textcircled{a}} \end{cases} \tag{A.3}$$

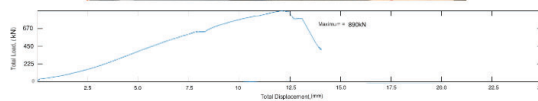
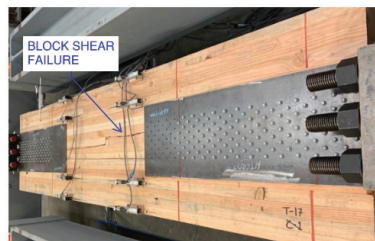
(b)

Figure 4: (a) NDS Appendix E block shear (group tear-out) equations. (b) Eurocode 5 Annex A block shear equations.

## 3 RESULTS AND DISCUSSION

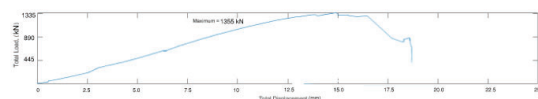
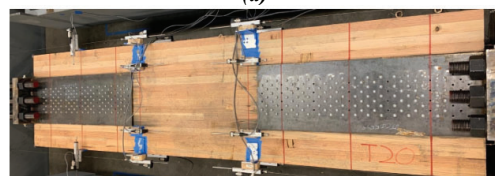
### 3.1 Summary of Results

The axial tension specimen test results for the smaller side-plated wood screw connections (type C4 per figure 1) aligned quite closely with calculated connection capacities based on the manufacturer published values, with load-displacement data indicating that ductile screw flexure was the dominant failure mode in those connections. However, the initial axial tension specimen tests for the medium and large connections (types C2, C3, C5, and C6 per figure 1) demonstrated block shear failures in the glulam beams at load levels significantly below calculations based on manufacturer published fastener shear capacity. After review of preliminary results, groups of (2) 10 mm diameter perpendicular-to-grain reinforcing screws were added at 150 mm spacing along the length of the larger side plate connections (C5 and C6) through the glulam beam, with the spacing of the wood screws in the side plates re-spaced to provide a 50 mm gap at reinforcing screw pair location. These reinforcing screws extended a minimum of 75 mm past rows of connection wood screws, as shown in figure 5 below, to increase resistance to glulam splitting and block shear.



LOAD VS DISPLACEMENT WITHOUT REINFORCING SCREWS

(a)



LOAD VS DISPLACEMENT WITH REINFORCING SCREWS

(b)

Figure 5: (a) tension specimen without reinforcing screws, showing load displacement curve (b) tension specimen with reinforcing screws, showing load displacement curve.

Subsequent tests of reinforced connection types C5 and C6 achieved significantly higher capacities more in-line with the capacities needed for the design and estimated by calculations. See figure 5 showing load vs deformation for the reinforced vs unreinforced connections. It was not feasible to add reinforcing screws for the specimens with the double plates slotted into the glulams (C2 and C3) due to inadequate width of the roughly 50 mm wide glulam sections each side of the plates.

Upon completion of physical load testing, the data was compiled and analysed, and the project team selected the double side plate connections with wood screws for use on the project due to their higher capacity, improved constructability, and lower cost. The test failure loads and calculated nominal design capacity for these connections is shown in figure 6. For design, the LRFD resistance factor of 0.65 was applied to these nominal capacities per NDS [5], and compared against factored loads from ASCE 7-16 [7]. The capacity for the wood portion of the wood connections was based upon the statistical analysis completed per ASTM D2915-17 [3], with the following equation: Avg Load – (Std. Dev. x K). The K factor is based on the one-sided tolerance limit for a normal distribution (with a 75% confidence level and a population content of 95%) which varies depending on the number of tests completed. This is the standard procedure

used for statistical analysis of wood connections in the US. Specimen failure loads and calculated nominal capacities for the connection types used in the project (types C4, C5 & C6) are illustrated in figure 6.

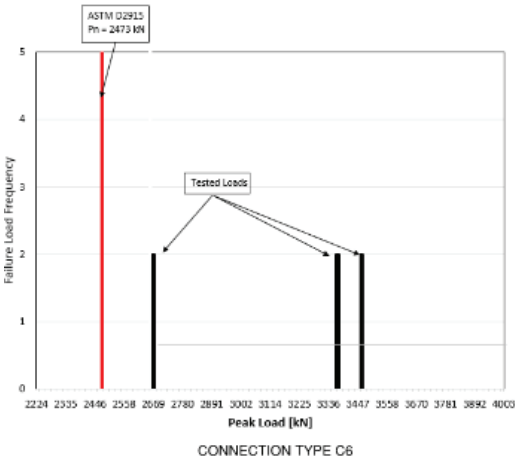
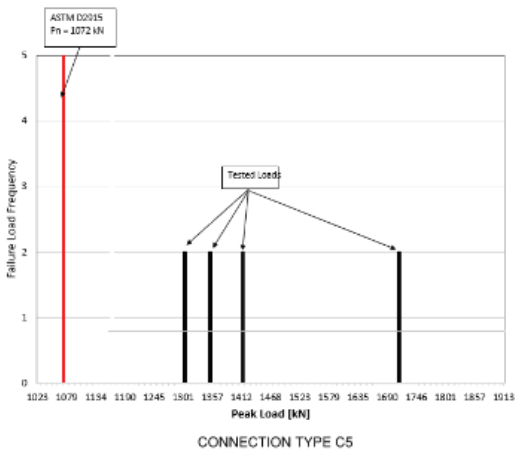
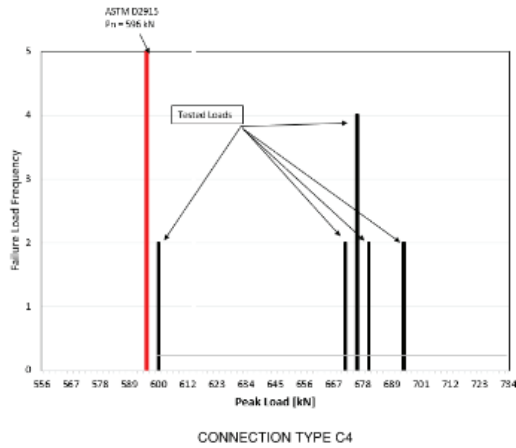


Figure 6: ASTM D2915-17 [3] test data and capacities

The failure loads indicated on figure 6 represent two data points since each tension specimen included two connections, one on each end. It should be noted that two vertical bars representing two specimens with very similar failure loads sometimes appear as a single, wider bar in figure 6. The majority of the tested failure loads are significantly larger than the nominal design capacity per ASTM D2915-17 [3]. However, for connection type C4 and C6, one outlier occurred with a failure load that was closer to the calculated nominal capacity.

The connection testing proved to be valuable in that it proved the connections could safely be used with a justifiable design capacity, with appropriate reinforcing. Additionally, for the actual project design conditions, where possible, the design was optimized such that bending of ductile steel plates in the connection assembly would be the controlling capacity, effectively limiting the load applied to the wood fasteners, to further ensure good behaviour in the event of an unforeseen overload.

### 3.2 Comparison of Test Data with NDS and Eurocode

For the smallest connection types, the failure mode appeared to be NDS [5] Mode IV fastener yielding, and the test results closely matched the calculated values utilizing the NDS equations (test values were approximately 10-20% higher than calculated values using NDS equations). The capacities utilizing the NDS equations were calibrated to the nominal LRFD capacity using a  $K_f$  of 3.32 and a  $\lambda$  of 1.0 (for short term, 10 min loading). None of the smallest connection types exhibited block shear or splitting failures, thus no reinforcing screws were added to the connections.

For the mid-size connection types utilizing the double plates slotted into the glulam with SDDs, the NDS greatly overpredicted the capacity of the connection, whereas Eurocode [6] only slightly overpredicted the capacity. The failure modes in these connection types were predominantly wood block-shear failures. If the Eurocode equation is used and only the shear portion is considered, the calculation closely predicts the tested values (less than 5% difference). However, if the tension portion of the equation is also considered, which in the mid-size connections results in a larger calculated capacity, the calculation moderately overpredicts the tested values (approximately 30%). The NDS equations overpredicted the capacity by approximately 80%. The initial mid-size connections utilizing the double side plates with wood screws similarly initially underperformed relative to calculated capacities, but after adding fully threaded reinforcing screws, the tested capacity more closely matched the calculated capacity.

For the largest connections utilizing the double plates slotted into the glulam with SDDs, the tested capacities were very closely predicted by both the NDS equations and the Eurocode equations. However, due to one outlier (that was significantly stronger than expected), the

capacity using the statistical analysis per ASTM D2915-17 [3] resulted in a capacity 30% lower than the equations predicted due to the increase in standard deviation. For the large connections using the double side plates and wood screws, with reinforcing screws, test capacities exceeded the capacity predicted by both the NDS and the Eurocode calculations. However, one outlier (which was significantly lower than the others), resulted in the capacity using the statistical analysis per ASTM D2915-17 being nearly equal to the code equation predictions.

See figure 7 below for a comparison of the calculated capacities and test values of specimen types.

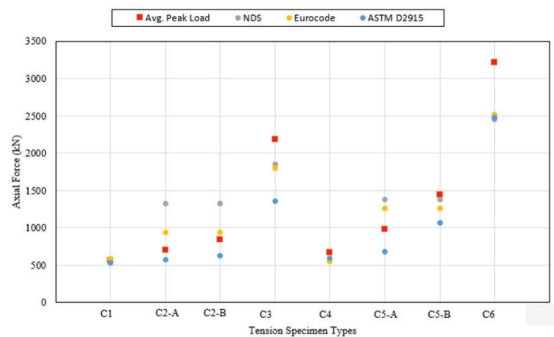


**Figure 7: Comparison of calculated versus tested capacities. Connection type C2-A and C2-B indicate connection type C2 with different distances from the last row of fasteners to the end of the glulam. Connection type C5-A and C5-B are both connection type C5 (with C5-A having no reinforcing screws and C5-B with reinforcing screws)**

### 3.3 Discussion

#### 3.3.1. Effect of reinforcing screws

Reinforcing screws passing through the connection area perpendicular to grain significantly improved the performance of the mid-size and larger connections by resisting block shear/splitting across the glulam wood grain. In the cases of the mid-size side plate connection, the capacity of the connections improved by approximately 50% after adding the reinforcing screws.

#### 3.3.2. Effect of moisture testing

See Section 2.2.2 for additional discussion on the specific moisture testing and cycling that was performed. The failure modes and capacities for moisture-cycled specimens were determined to not be statistically different from non-moisture-cycled specimens. As discussed in Section 1.1, the connection geometry was developed per the NDS [5] recommendation of 150 mm maximum dimension of outer rows of fasteners perpendicular to grain to prevent perpendicular to grain splitting due to shrinkage restraint. Tests of the moisture cycled specimens showed no indication of a reduction in capacity with the tested configurations, indicating the NDS recommendations appear to be appropriate for the MC variations considered.

## 4 CONCLUSIONS

### 4.1 Summary

Load testing of the initial design of the medium- and large-size connections exhibited brittle block shear/group tear-out failure modes which were not adequately predicted by calculations using the National Design Specification (NDS) for Wood Construction [5]. Calculations using Eurocode 5 [6] provided better predictions. This is a result of the NDS equations considering the sum of the resistance from both the shear and tension portions of a potential failure perimeter whereas the Eurocode equations only taking the larger of the shear or tension portion capacity.

The addition of reinforcing screws perpendicular to grain prevented block shear/group tear-out failure modes and allowed the medium- and large-size connections to realize the ultimate capacity and ductility of the dowel-type fasteners. That ultimate capacity of reinforced connections was reasonably well predicted by NDS equations.

Moisture cycling of connection specimens prior to load testing did not discernibly change the failure modes or capacities compared to connection specimens which were load tested without prior moisture cycling. This may support the conclusion that NDS recommendations for limiting the maximum distance perpendicular to grain between outer rows of fasteners in a given connection are sufficient for the moisture content variations considered in this research. Furthermore, moisture cycle testing on connection specimens provided specific criteria for moisture content management and control of the project connections throughout construction.

Successful physical testing of the glulam moment connections for the TCORE project made possible the long spans/cantilever conditions and resulting large axial tension/compression force couple demands. Although calculation-based approaches were available in the U.S. codes and standards, load testing was pursued by the project team to provide greater assurance and economy of the design. It also resulted in streamlined jurisdictional approval of these connections. As of the end of 2022, all connections had been installed in the over 400 glulam beams present in the roof, and the majority of the roof structure had been erected over the terminal.

### 4.2 Impact on Future Research and Codes

Based on the results of the connection load testing for this project, it is suggested that a thorough literature review be performed to specifically investigate block shear/group tear-out failure modes, particularly in large connection geometries. If the available literature is lacking or inconclusive, additional load testing may be necessary to determine the capacity of these failure modes. Ultimately, the available literature and any supplemental testing could inform changes to the block shear/group tear-out equations in the NDS [5] and Eurocode [6], especially if,

as identified in this research, the existing equations are not conservative. Finally, in this research, reinforcing screws installed perpendicular to grain were shown to prevent the development of block shear/group tear-out failure modes. However, little to no guidance exists in NDS or Eurocode for the appropriate design (e.g., diameter, length and spacing) of such reinforcing screws.

#### ACKNOWLEDGEMENT

The authors would like to thank the many individuals at ZGF Architecture (Architect of Record), Swinerton Mass Timber (mass timber subcontractor), and the Port of Portland (owner) who contributed to the glulam connection testing and the TCORE project in general. The authors would also like to thank the laboratory staff at the iSTAR Laboratory at Portland State University and at the environmental chamber at Oregon State University. Finally, the authors would like to acknowledge the significant, sometimes herculean, contributions of our colleagues at KPFF in making this research and project a success.

#### REFERENCES

- [1] Zimmerman, R.B. and Pitt, C. (2022). Seismic Isolation of the Terminal Core Roof at the Portland International Airport. In *Proceedings of the 17<sup>th</sup> World Conference on Seismic Isolation, Energy Dissipation and Active Vibration Control of Structures*, Anti-Seismic Systems International Society (ASSISi), Turin, Italy, September 11-16, 2022.
- [2] ASTM International. (2020). *Standard Test Methods for Mechanical Fasteners in Wood, ASTM D1761-12*. West Conshohocken, PA.
- [3] ASTM International. (2022). *Standard Practice for Sampling and Data-Analysis for Structural Wood and Wood Based Products, ASTM D2915-17*. West Conshohocken, PA.
- [4] ASTM International. (2018). *Standard Test Method for Evaluating Dowel-Bearing Strength of Wood and Wood Based Products, ASTM D5764-97a*. West Conshohocken, PA.
- [5] American Wood Council. (2018). *National Design Specification for Wood Construction*. Leesburg, VA.
- [6] European Committee for Standardization. (2008). *Eurocode 5: Design of Timber Structures – Part 1-1: General – Common Rules and Rules for Buildings*. Rue De Stassart, 36 B-1050 Brussels.
- [7] American Society of Civil Engineers/Structural Engineers Institute. (2016). *Minimum Design Loads and Associated Criteria for Buildings and Other Structures*. Reston, VA.